Talanta 125 (2014) 366–371

Contents lists available at ScienceDirect

Talanta

journal homepage: www.elsevier.com/locate/talanta

Non-enzymatic glucose sensors based on controllable nanoporous gold/copper oxide nanohybrids

Xinxin Xiao [a], Meng'en Wang [a], Hui Li [a], Yichuan Pan [b], Pengchao Si [a,*]

[a] Key Laboratory for Liquid–Solid Structural Evolution and Processing of Materials, Ministry of Education, School of Materials Science and Engineering, Shandong University, Jinan 250061, People's Republic of China

[b] School of Mechanical Engineering, Shandong Jiaotong University, Jinan 250023, People's Republic of China

ARTICLE INFO

Article history:
Received 25 October 2013
Received in revised form
11 March 2014
Accepted 14 March 2014
Available online 21 March 2014

Keywords:
Nanoporous gold
Copper oxide
Non-enzymatic
Glucose

ABSTRACT

A kind of dealloyed nanoporous gold (NPG)/ultrathin CuO film nanohybrid for non-enzymatic glucose sensing has been prepared by a simple, in-situ, time-saving and controllable two-step electrodeposition. The three-dimensional and bicontinuous nanoporous structure of the nanocomposites have been characterized by scanning electron microscope (SEM) and transmission electron microscopy (TEM), and the electrochemical tests have been estimated by cyclic voltammetry and single potential step chronoamperometry (SPSC). The optimal NPG/CuO electrode exhibits great electrocatalytic activity towards glucose oxidation and also shows obvious linear response to glucose up to 12 mM with a high sensitivity of 374.0 μA cm^{-2} mM^{-1} and a good detection limit of 2.8 μM ($S/N=3$), as well as strong tolerance against chloride poisoning and interference of ascorbic acid and uric acid.

1. Introduction

The development of glucose sensors is of a vital importance in diabetes control, food industry and bioprocess monitoring [1–3]. Since Clark and Lyons developed the first enzyme electrode in the 1960s [4], there have been many impressive advances in the design and use of glucose biosensors based on the superior selectivity and non-toxicity of enzyme based electrodes [1,5]. However, more critical demands, such as withstanding with harsh conditions (e.g. high operating temperature), relatively long shelf life and eventual low cost, have proposed new challenges to enzyme based glucose sensors. Accordingly, non-enzymatic glucose sensors utilizing metal and metal oxide nanomaterials have attracted numerous attentions in the recent years [6–9], due to their low cost and promising capabilities including long stability, rapid response, ultra-low detection limit and great sensitivity even as high as mA mM^{-1} cm^{-2} [10,11]. Among them, CuO has been widely studied for non-enzymatic glucose sensing as a result of its ease of synthesis, low cost and high electroactivity, especially good poisoning tolerance [10,12]. Various nanostructured CuO with different morphologies, such as nanowires [13], nanoplatelets [14], nanospheres [15], nanorods [16], and nanofibres [17,18], have been proposed. A fundamental conflict for CuO based electrodes remaining to be addressed is that, as a p-type semiconductor, large loading of CuO would generate high response signal; however, accompanied by increased charge transfer resistance. To deal with this, many efforts have been made to develop nanocomposite electrodes like CuO/multiwalled carbon nanotubes (MWCNTs) [19], CuO/graphene [20] and CuO nanoneedle/graphene/carbon nanofiber [21] in order to generate a synergistic effect. It should also be noted that the unsupported nanostructures of CuO are somewhat unstable during the long electrochemical procedure, as a result of undesirable segregation and growth, giving restriction in the capability of glucose oxidation [10]. Additionally, CuO based electrodes in previous work display the ultrahigh sensitivities, the linear range is relatively narrow within the realm of blood glucose concentration in human body (i.e. 2–10 mM), which is limited in the application of in-vivo and online monitoring. Therefore, exploring novel materials and new technology are imperative for non-enzymatic glucose sensors.

Recently, dealloyed nanoporous gold (NPG) is a truly self-supported material with three-dimensional and bicontinuous nanoporous structure [22,23]. The composites of NPG and metal oxides, such as NPG/MnO_2 [24] and NPG/RuO_2 [25], have been achieved as high-performance electrochemical supercapacitors due to their promising electron transfer capability and high stability. Most recently, Lang and his coworkers have reported NPG micro-electrodes decorated with Co_3O_4 nanoparticles by the hydrothermal method, which exhibited ultrahigh electrocatalytic activity towards glucose oxidation [26]. In this paper, a simple, time-saving and

* Corresponding author.
E-mail address: pcsi@sdu.edu.cn (P. Si).

http://dx.doi.org/10.1016/j.talanta.2014.03.030
0039-9140/

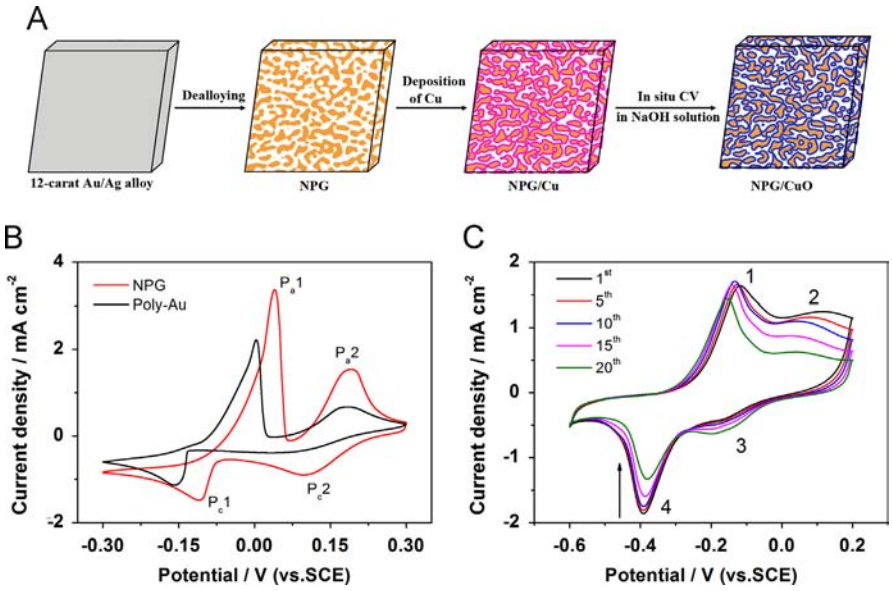

Fig. 1. (A) Schematic drawing of the synthesis of NPG/CuO electrode. (B) CVs of NPG (red) and poly-Au (black) in 0.1 M KCl solution containing 10 mM $CuCl_2$ at 10 mV s^{-1}. (C) CVs of NPG/Cu electrode in 0.1 M NaOH at 100 mV s^{-1}. (For interpretation of the references to color in this figure legend, the reader is referred to the web version of this article.)

controllable two-step electrodeposition has been adopted to fabricate NPG/CuO hybrid electrodes. Cu is firstly electrodeposited onto the NPG surface under a constant potential in $CuCl_2$ solution and electrochemically oxidized into CuO via cyclic voltammetry in alkaline solution [27] (Fig. 1A). TEM and SEM results show that the NPG preserves its original bicontinuous nanoporous structure and the CuO film is ultrathin (with a thickness of ~5 nm). It is expected that the composites of NPG and ultrathin CuO film would possess enhanced electrochemical activities, improved biocompatibility, larger accessible surface area and promoted electron transfer. The detailed electrochemical behaviors show NPG/CuO electrode that serves as an excellent sensitive non-enzymatic glucose sensor with a wider linear range compared to conventional CuO based on the electrodes reported in the previous literatures.

2. Experimental section

2.1. Chemicals and apparatus

Potassium chloride (KCl, 99.99%), cupric chloride dihydrate ($CuCl_2 \cdot 2H_2O$, 99.99%), sodium hydroxide (NaOH, 99.99%), sodium chloride (NaCl, 99.99%) and β-D-glucose (99.99%) were supplied by Aladdin (China). Ascorbic acid (AA, 99%), uric acid (UA, 99%), sulfuric acid (H_2SO_4, 98%) and nitric acid (HNO_3, 65%) were ordered from Shanghai Sinopharm Chemical Co., Ltd. (Shanghai, China). All chemicals were used as received without any further purification. Ultrapure water with a resistivity >18.25 MΩ cm^{-1} was obtained from a UPH-IV ultrapure water purifier (Chengdu Ultrapure Technology Co., Ltd, China).

All the electrochemical experiments were performed on a LK2005A electrochemical workstation system (Lanlike Company, Tianjin). A classical three-electrode cell was used, with a Pt wire counter electrode, NPG/CuO working electrode, and a saturated calomel reference electrode (SCE). All potentials were reported with respect to SCE.

Morphology characterization of NPG and NPG/CuO samples was performed by field emission scanning electron microscope (FESEM, Hitachi SU-70) and transmission electron microscopy (TEM; JEOL JEM-2100). The SEM was also equipped with an energy dispersive X-ray spectroscopy (EDX) system for elemental analysis.

2.2. Preparation of NPG

NPG sheets were fabricated by dealloying 100-nm-thick Au/Ag leaves (12-carat, Sepp Leaf Products, New York) in concentrated HNO_3 for 30 min at 30 °C as in the previous work [23]. After carefully cleaning with ultrapure water, the NPG films were placed onto pre-polished glassy carbon electrode (GCE) with a diameter of 4 mm and redundant parts were removed carefully with toothpicks. Before electrodeposition, cyclic voltammetry of NPG in 1 M H_2SO_4 were carried out to create high surface areas.

2.3. In situ electrodeposition of CuO onto NPG/CuO electrodes

NPG/CuO composite electrodes were synthesized by the electrodeposition of CuO onto the surface of NPG electrodes using a simple film plating/potential cycling procedure [27] (Fig. 1A). In brief, a constant deposition potential was applied to the NPG electrode in 0.1 M KCl solution containing 10 mM $CuCl_2$ (pre-bubbled with N_2 to remove O_2). The optimized deposition time here was 120 s. After rinsing with ultrapure water, the NPG/Cu was oxidized in situ into NPG/CuO in 0.1 M NaOH solution by cycling potential from -0.6 to 0.2 V at 100 mV s^{-1} for 20 cycles. For comparison, similar strategy was used to grow CuO onto a polished polycrystalline gold electrode, denoted as Au/CuO.

3. Results and discussion

3.1. NPG/CuO preparation

Fig. 1B shows typical cyclic voltammograms (CVs) of NPG and normal polycrystalline gold (poly-Au) in 10 mM $CuCl_2$ solution. As for NPG, two pairs of redox peaks, P_a1/P_c1 and P_a2/P_c2, indicating two different deposition/stripping processes, can be found. According to the previous work [28–30], P_c1/P_a1 is associated to the redox pair of freely Cu^{2+} and deposited Cu from the overpotential deposition (OPD), as a diffusion controlled process. Meanwhile, P_c2/P_a2 is due to the redox Cu underpotential deposition (UPD) and stripping of Cu on the gold electrode, being a surface-constrained electrochemical process. Compared with poly-Au electrode, enhancements of current density on the NPG electrode are much more

profound for the Cu UPD (P_c2) than that of Cu OPD (P_c1). This is because the inner pores of NPG give no contribution to the diffusion controlled process but have a great effect on the surface constrained process. Strikingly, the potential of the OPD (P_c1) on the NPG electrode is approximately 53 mV more positive than that of poly-Au electrode, which is probably the result of the unique crystal planes of NPG [31].

Fig. 1C displays CVs of as-prepared NPG/Cu in 0.1 M NaOH solution. Two pairs of redox peaks can be seen in the range of −0.6 and 0.2 V, which are attributed to a series in-situ redox transitions from Cu(0) to CuO [32]. Peak 1 and peak 2 in the anodic scans are possibly due to the transition of Cu(0)/Cu_2O and CuOH/CuO, respectively. Correspondingly, the cathodic peaks, 3 and 4, are due to the conversion of CuO/Cu_2O(CuOH) and Cu_2O(CuOH)/Cu (0) respectively. Obvious decrease of the cathodic peak (peak 4) with the cyclic potential proceeding, caused by the increase of impedance, affords a solid evidence of the CuO formation on the electrode surface. The possible mechanism can be expressed as follows [27]:

$$Cu + OH^- \leftrightarrow CuOH + e^- \quad (1)$$

$$2CuOH + OH^- \leftrightarrow Cu_2O + 2H_2O \quad (2)$$

$$Cu_2O + 2OH^- \leftrightarrow 2CuO + H_2O + 2e^- \quad (3)$$

3.2. Optimization of the hybrid electrode for glucose sensing

The two-step electrodeposition of CuO thin film onto NPG electrode is a controllable process (Fig. 1A). In other words, the film thickness can be adjusted by varying the deposition conditions (i.e. potentials and durations), which would exhibit different response signals towards glucose. Effects of deposition potential and deposition time in the first step on the response to 5 mM glucose in 0.1 M NaOH solution are shown in Fig. 2A and B, respectively. The optimal potential and time is determined to be −0.2 V and 120 s. According to the aforementioned results (Fig. 1B), −0.2 V is in the OPD regime, wherein bulk deposition occurs and nano-clusters start to grow. While in the UPD region, only monolayer or sub-monolayer is formed [33], leading to not enough electrocatalytic active CuO exists. On the other hand, as a semiconductor metal oxide, the lower deposition potential causes the thicker CuO film, which would decrease the capability of electron transfer during electrocatalysis and negate the relative advantages (e.g. large surface/volume ratio) of NPG. This is also the reason why the optimal deposition time is not longer than 120 s. Moreover, once too much Cu deposited, exfoliation of the grown film can be observed in the second step during continuous potential scanning in alkaline solution.

3.3. Electrocatalytic oxidation of glucose of the NPG/CuO

Cyclic voltammetry in the potential window from 0.2 to 0.7 V at 100 mV s^{-1} in 0.1 M NaOH solution with presence of 5 mM glucose is used to evaluate the catalytic activities of bare NPG and NPG/CuO electrodes (Fig. 2C). In a blank solution, neither the bare NPG nor NPG/CuO electrode shows oxidation peaks. With the addition of glucose, the NPG/CuO electrode shows remarkable oxidation of glucose with an initial potential of ca. +0.25 V and a broad peak at ca. +0.45 V, while the current signal is relatively lower on the bare NPG electrode. Compared to Au/CuO electrode prepared in the same route, the NPG/CuO electrode shows much higher response to glucose (Fig. S1). Supplementary experiments in phosphate buffer solution (pH 7.5) show no response of NPG/CuO electrode (data not shown), corroborating the significance of OH^- ions for the process. As given in the previous report bare NPG shows electrocatalytic activity toward glucose oxidation in a nearly neutral PBS solution (pH 7.4) [34], therefore, herein NPG has been completely coated with CuO and only the CuO thin film contributes the oxidation. These results illustrate that the NPG/CuO hybrid has significantly improved the electrocatalytic ability, due to the combination of both large surface area of the NPG and the electrocatalytic active site providing by the ultrathin CuO film.

In order to deeply understand the oxidation process, different scan rates have been employed on the NPG/CuO electrode in 5 mM glucose solution. As shown in Fig. 2D, with the increase of scan rate, the anodic peak current rises linearly and the anodic peak potential shifts positively, indicating that the electro-oxidation of glucose on NPG/CuO is a surface adsorption/selectivity and diffusion controlled process. An OH^- ion involved mechanism of electro-oxidation of glucose in alkaline electrolyte can be described as follows [14,35]:

$$CuO + OH^- \rightarrow CuOOH + e^- \quad (4)$$

or

$$CuO + H_2O + 2OH^- \rightarrow Cu(OH)_4{}^- + e^- \quad (5)$$

$$Cu(III) + Glucose + e^- \rightarrow Gluconolactone + Cu(II) \quad (6)$$

$$Gluconolactone \rightarrow Gluconic\ acid\ (hydrolysis) \quad (7)$$

Additionally, no obvious change can be seen from the CV after removing dissolved oxygen from the solution by bubbling with N_2 (data not shown), implying the oxygen-independent behaviors of the glucose oxidation process.

3.4. Morphology characterization of the NPG/CuO electrode

Fig. 3A and B shows the SEM images of bare NPG and NPG/CuO nanocomposite. It is clearly seen that bare NPG displays unique bicontinuous nanoporous structure (Fig. 3A), with a homogeneous pore/ligament size of ~30 nm. After the deposition of CuO on the NPG surface, the original nanoporous structure still retains. Fig. 3E shows an EDX spectrum for the as-fabricated samples supported on a carbon conductive adhesive tape. The existence of elements Cu and O also help us to make sure the formation of CuO. For further characterizing the morphology and thickness of CuO film, TEM images are taken at the edge of the freshly prepared sample (Fig. 3C and D). The average thickness of the uniform grown CuO is around 5 nm, indicating the large surface area and high surface energy for glucose oxidation. The selected area electron diffraction (SAED) pattern of CuO indexed as $(\bar{3}11)$ and (002) planes is shown in the inset image of Fig. 3C, suggesting that the CuO film is polycrystalline. TEM image in Fig.3D shows an interplanar spacing 0.275 nm corresponded to $(\bar{1}10)$ plane of the CuO (JCPDS 45-0937).

3.5. Amperometric response to glucose

According to the CV results, +0.4 V is selected as the constant detecting potential to evaluate the senor behavior, which is relatively low to avoid interference from electroactive species. The classical amperometric response of the NPG/CuO electrode at the constant potential to successive additions of 1 mM glucose in 0.1 M NaOH is shown in Fig. 4A. The NPG/CuO electrode generate plateau current signal linearly increasing along with glucose concentration increment, and reach steady-state within 10 s. As observed in the calibration curve (Fig. 4B), the proposed electrode gives a high sensitivity of 374.0 μA cm^{-2} mM^{-1} with a correlation coefficient of 0.99918. The upper of the linear range is 12 mM and the limit of detection is 2.8 μM at a signal-to-noise ratio of 3. It is inferred that the high sensitivity and wide linear range of the

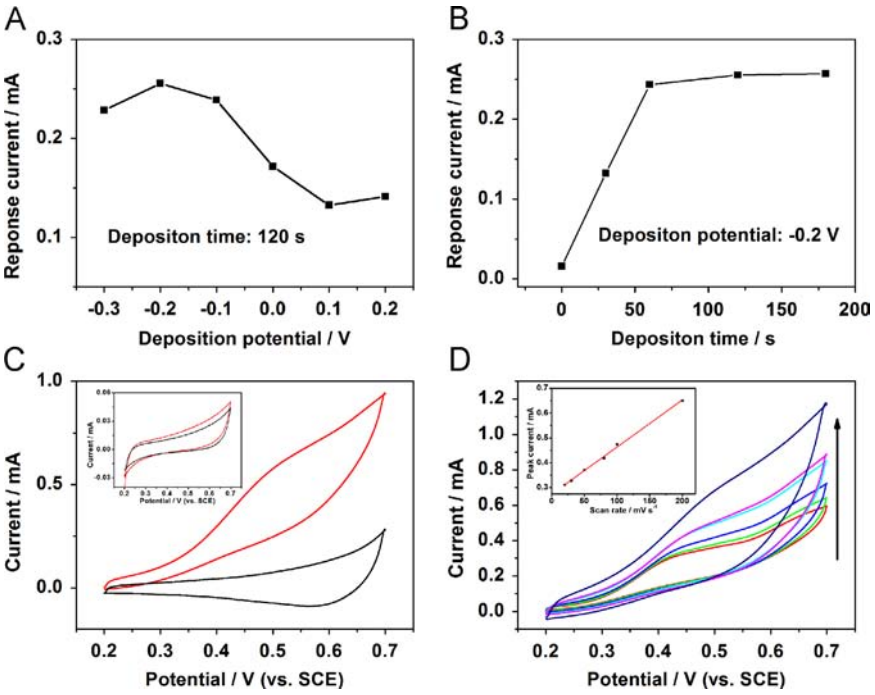

Fig. 2. Effects of the deposition potential (A) and deposition time (B) on the response to 5 mM glucose of NPG/CuO electrode. (C) CVs of NPG electrode (insert), NPG/CuO electrode ran at 100 mV s^{-1} in 0.1 M NaOH in the absence (black) and presence (red) of 5 mM glucose. (D) CVs of the NPG/CuO electrode in 0.1 M NaOH containing 5 mM glucose at different scan rate from 20 to 200 mV s^{-1}. Inset shows the anodic peak current vs. scan rate. (For interpretation of the references to color in this figure legend, the reader is referred to the web version of this article.)

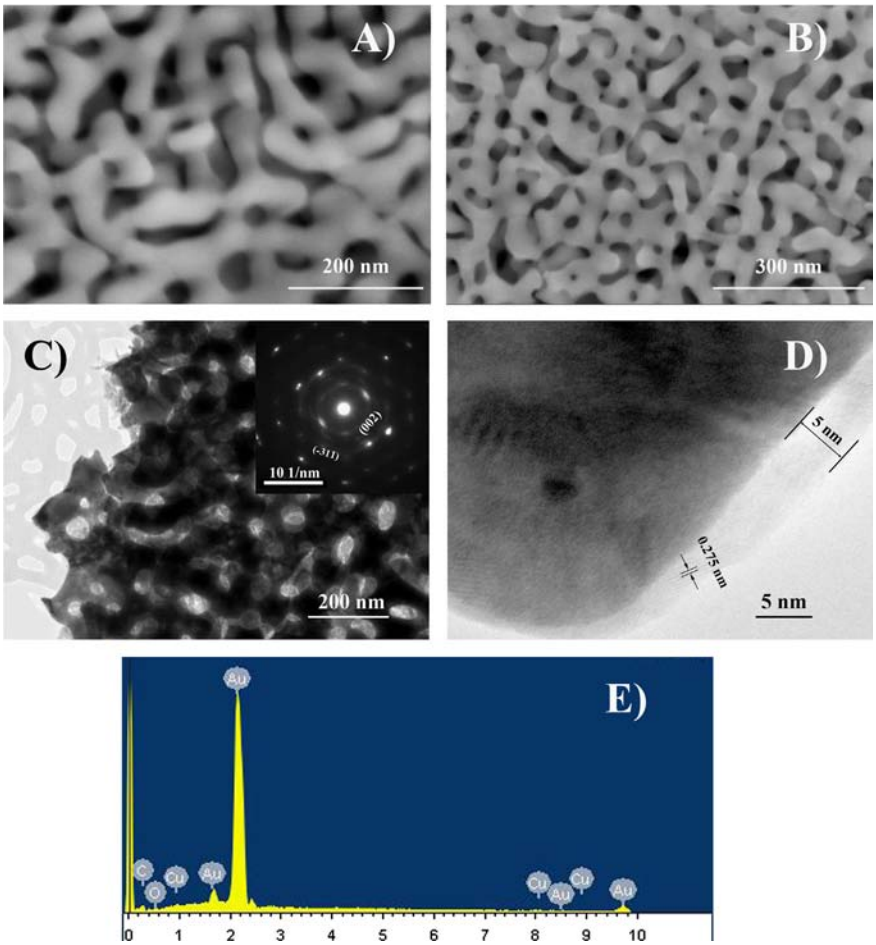

Fig. 3. SEM images of NPG (A) and NPG/CuO (B). (C, D) TEM images of NPG/CuO. (E) EDX spectrums of the NPG/CuO composite. The inset in C is a SAED pattern of the corresponding sample.

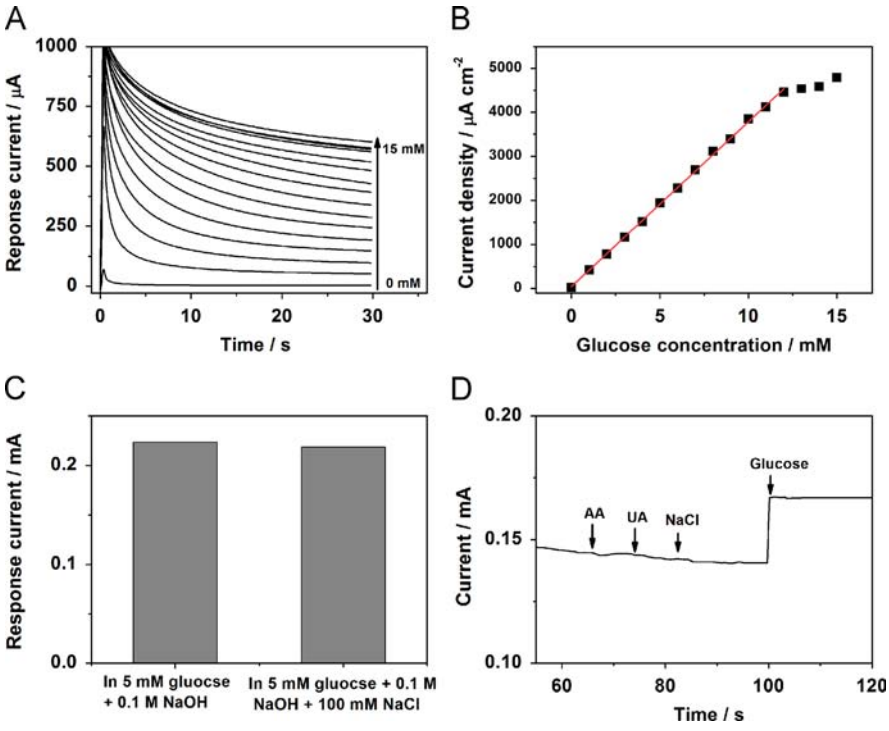

Fig. 4. (A) Current–time plots of NPG/CuO with various glucose concentrations in 0.1 M NaOH solution at 0.4 V (vs. SCE). (B) Calibration plot of the NPG/CuO electrode. (C) Responses of the sensor to 5 mM glucose in 0.1 M NaOH solution with and without 100 mM NaCl. (D) Responses of the sensor in 0.1 M NaOH with the successive addition of 0.1 mM AA, 0.1 mM UA, 1 mM NaCl and 3 mM glucose.

Table 1
Comparison of sensor behavior of the NPG/CuO electrode with other reported CuO or NPG based non-enzymatic glucose sensors.

Reference	Electrodes	Reference electrode	Applied potential (V)	Sensitivity ($\mu A\ cm^{-2}\ mM^{-1}$)	Linear range (up to, mM)	Detection limit (μM)
(This work)	NPG/CuO	SCE	0.4	374.0	12	2.8
[15]	CuO nanospheres	Ag/AgCl	0.6	404.53	2.5	1.0
[16]	CuO nanorods	Ag/AgCl	0.6	371.4	8.0	4.0
[20]	CuO–graphene hybrid	SCE	0.59	1360.0	4	0.7
[19]	CuO–MWCNTs hybrid	Ag/AgCl	0.55	2190.0	3.0	0.8
[37]	Cu_xO/polypyrrole/Au	SCE	0.6	232.22	8.0	6.2
[38]	Hydrogen bubble dynamic template synthesized NPG	SCE	0.35	11.8	10.0	5.0
[34]	Dealloyed NPG	Ag/AgCl	0.3	20.1	18.0	3.0
[39]	Three-dimensional gold	SCE	−0.3	46.6	10.0	3.2
[40]	NPG–Ru hybrid	SCE	−0.1	240.0	6.0	1.7

NPG/CuO would owe to its inherent unique bicontinuous nanoporous structure [26], which significantly enhance the diffusion of glucose and accessibility to the ultrathin layer of CuO. The sensor behavior of NPG/CuO electrode has been compared with other reported CuO or NPG based non-enzymatic glucose sensors in Table 1. Its sensitivity is comparative with other nanostructures of CuO and their hybrid based materials and higher than NPG based sensors from the comparative data. Moreover, when comparing with CuO prepared with other kinds of routes, the proposed strategy here, by in situ electrodepositing CuO thin film onto an open-structured NPG electrode, is relatively controllable, easy-operable and high-performing.

It is noteworthy that the proposed sensor exhibits relatively wider detecting linear range (up to 12 mM, i.e. the active CuO is fully utilized at 12 mM or higher in a quiescent solution) than that of most CuO or NPG based sensors (Table 1), making it suitable for reliable practical applications in future as the realm of blood glucose concentration in human body is 2–10 mM) [6]. Analogous to the enzymatic sensors, which show the characteristics of the Michaelis–Menten kinetics [36], the steady-state current for glucose detection that approaches a limit depends on the active sites of catalyst (CuO here) and the ability to oxidize glucose under specific diffusional conditions (in a quiescent solution here).

3.6. Anti-interference test

Inhibition in terms of competitive adsorption of chloride anions is not negligible for glucose sensing, since the chloride concentration is as high as around 100 mM in the blood [6]. Thus, amperometric responses of the NPG/CuO electrode to 5 mM glucose in 0.1 M NaOH solution are examined in the absence and presence of 100 mM NaCl. It can be seen from Fig. 4C that the current signal is slightly affected in the presence of high concentration of chloride ions.

Selectivity is another important parameter for a glucose sensor, which has been investigated by adding 0.1 mM AA and 0.1 mM UA as representative in this work, considering the interfering species ratio of ~30 [17]. Comparing with the injection of 3 mM glucose,

Table 2
Glucose detection of real samples.

Sample	Biochemical analyzer (mM)	NPG-DTDPA-GOx[a] (mM)	RSD (%)
1	5.41	5.18	2.87
2	4.62	4.60	3.62
3	4.76	4.83	1.25

[a] Each sample has been measured in triplicate.

no significant current change on the NPG/CuO electrode is observed (Fig. 4D). In addition, the NPG/CuO electrode sensor can still demonstrate good sensitivity and wide detection liner range in the presence of UA and AA, confirming its high selectivity and reliable anti-interference property.

3.7. Determination in real samples

The NPG/CuO electrode has been applied to detect glucose of human serum samples with a 100-fold dilution in 0.1 M NaOH solution at +0.4 V (vs. SCE), in order to verify its applicability in real sample analysis. Compared with those measured by a biochemical analyzer (Cobas 8000 analyzer, Roche Diagnostics, Germany), the calculated results are summarized in Table 2. The results are demonstrated to be acceptable with the data collected by the commercial analyzer, revealing the potential of the proposed electrode for practical application.

4. Conclusions

Three-dimensional NPG/CuO hybrid electrodes, which display high electrocatalytic activity to glucose oxidation, have been developed by a simple, fast and reliable two-step electrodeposition approach. The film thickness of CuO on NPG electrode can be controlled as thin as around 5 nm via electrochemical deposition. The NPG/CuO based non-enzymatic glucose sensor exhibits a high sensitivity (374.0 $\mu A\ cm^{-2}\ mM^{-1}$), a wide linear range (up to 12 mM glucose) and good anti-interference ability, which is promising for glucose sensing in food and the human blood. This strategy provides a new perspective of designing of nanoporous metal/metal oxide nanocomposites for high performance sensors.

Acknowledgments

This work was sponsored by the National Natural Science Foundation of China (NSFC, No. 51301096), Shandong Provincial Natural Science Foundation (ZR2013EMQ012), Project Nos. 31370056431211 and 31370070614018 (2010TB018) from Shandong University and the National 973 Program Project of China (2012CB932800). We also appreciate Prof. Yi Ding for his kind support.

Appendix A. Supplementary material

Supplementary data associated with this article can be found in the online version at http://dx.doi.org/10.1016/j.talanta.2014.03.030.

References

[1] J. Wang, Chem. Rev. 108 (2008) 814–825.
[2] L. Liu, M. Shao, S.-T. Lee, J. Nanoeng. Nanomanuf. 2 (2012) 102–111.
[3] A. Zhang, D. Wheeler, Y. Ling, G. Wang, X. Yang, B. Vilozny, B. Singaram, C. Gu, Y. Li, Sci. Adv. Mater. 4 (2012) 1047–1054.
[4] L.C. Clark, C. Lyons, Ann. N. Acad. Sci. 102 (1962) 29–45.
[5] A. Heller, B. Feldman, Chem. Rev. 108 (2008) 2482.
[6] K.E. Toghill, R.G. Compton, Int. J. Electrochem. Sci. 5 (2010) 1246–1301.
[7] S. Park, H. Boo, T.D. Chung, Anal. Chim. Acta 556 (2006) 46–57.
[8] Y. Zhang, L. Su, K. Lubonja, C. Yu, Y. Liu, D. Huo, C. Hou, Y. Lei, Sci. Adv. Mater. 4 (2012) 825–831.
[9] K. Singh, A. Umar, A. Kumar, G. Chaudhary, S. Singh, S. Mehta, Sci. Adv. Mater. 4 (2012) 994–1000.
[10] S.K. Meher, G.R. Rao, Nanoscale 5 (2013) 2089–2099.
[11] G.M. Wang, X.H. Lu, T. Zhai, Y.C. Ling, H.Y. Wang, Y.X. Tong, Y. Li, Nanoscale 4 (2012) 3123–3127.
[12] J. Wang, W.D. Zhang, Electrochim. Acta 56 (2011) 7510–7516.
[13] Z.J. Zhuang, X.D. Su, H.Y. Yuan, Q. Sun, D. Xiao, M.M.F. Choi, Analyst 133 (2008) 126–132.
[14] H. Wei, J.J. Sun, L. Guo, X. Li, G.N. Chen, Chem. Commun. (2009) 2842–2844.
[15] E. Reitz, W.Z. Jia, M. Gentile, Y. Wang, Y. Lei, Electroanalysis 20 (2008) 2482–2486.
[16] X. Wang, C.G. Hu, H. Liu, G.J. Du, X.S. He, Y. Xi, Sens. Actuators B: Chem. 144 (2010) 220–225.
[17] F. Cao, J. Gong, Anal. Chim. Acta 723 (2012) 39–44.
[18] G. Liu, B. Zheng, Y. Jiang, Y. Cai, J. Du, H. Yuan, D. Xiao, Talanta 101 (2012) 24–31.
[19] J. Yang, L.C. Jiang, W.D. Zhang, S. Gunasekaran, Talanta 82 (2010) 25–33.
[20] L. Luo, L. Zhu, Z. Wang, Bioelectrochemistry 88 (2012) 156–163.
[21] D. Ye, G. Liang, H. Li, J. Luo, S. Zhang, H. Chen, J. Kong, Talanta 116 (2013) 223–230.
[22] Y. Ding, M.W. Chen, MRS Bull. 34 (2009) 569–576.
[23] X. Xiao, M.e. Wang, H. Li, P. Si, Talanta 115 (2013) 1054–1059.
[24] X.Y. Lang, A. Hirata, T. Fujita, M.W. Chen, Nat. Nanotechnol. 6 (2011) 232–236.
[25] L.Y. Chen, Y. Hou, J.L. Kang, A. Hirata, T. Fujita, M.W. Chen, Adv. Energy Mater. 3 (2013) 851–856.
[26] X.Y. Lang, H.Y. Fu, C. Hou, G.F. Han, P. Yang, Y.B. Liu, Q. Jiang, Nat. Commun. 4 (2013, 2169).
[27] W.Z. Le, Y.Q. Liu, Sens. Actuat. B: Chem. 141 (2009) 147–153.
[28] D.W.M. Arrigan, T. Iqbal, M.J. Pickup, Electroanalysis 13 (2001) 751–754.
[29] E. Garfias-García, M. Romero-Romo, M.T. Ramírez-Silva, M. Palomar-Pardavé, Int. J. Electrochem. Sci. 7 (2012) 3102–3114.
[30] J.F. Huang, B.T. Lin, Analyst 134 (2009) 2306–2313.
[31] T. Fujita, P.F. Guan, K. McKenna, X.Y. Lang, A. Hirata, L. Zhang, T. Tokunaga, S. Arai, Y. Yamamoto, N. Tanaka, Y. Ishikawa, N. Asao, Y. Yamamoto, J. Erlebacher, M.W. Chen, Nat. Mater. 11 (2012) 775–780.
[32] A.M. Castro Luna De Medina, S.L. Marchiano, A.J. Arvia, J. Appl. Electrochem. 8 (1978) 121–134.
[33] E. Herrero, L.J. Buller, H.D. Abruña, Chem. Rev. 101 (2001) 1897–1930.
[34] L.Y. Chen, X.Y. Lang, T. Fujita, M.W. Chen, Scr. Mater. 65 (2011) 17–20.
[35] J.M. Marioli, T. Kuwana, Electrochim. Acta 37 (1992) 1187–1197.
[36] R.A. Kamin, G.S. Wilson, Anal. Chem. 52 (1980) 1198–1205.
[37] F. Meng, W. Shi, Y. Sun, X. Zhu, G. Wu, C. Ruan, X. Liu, D. Ge, Biosens. Bioelectron. (2012, 141-147).
[38] Y. Li, Y.Y. Song, C. Yang, X.H. Xia, Electrochem. Commun. 9 (2007) 981–988.
[39] Y. Bai, W.W. Yang, Y. Sun, C.Q. Sun, Sens. Actuat. B: Chem. 134 (2008) 471–476.
[40] J.H. Shim, A. Cha, Y. Lee, C. Lee, Electroanalysis 23 (2011) 2057–2062.